Communication

Protonation of the Acidic Residues in the Transmembrane Cation-Binding Sites of the Ca Pump

Yuji Sugita, Naoyuki Miyashita, Mitsunori Ikeguchi, Akinori Kidera, and Chikashi Toyoshima

J. Am. Chem. Soc., **2005**, 127 (17), 6150-6151• DOI: 10.1021/ja0427505 • Publication Date (Web): 07 April 2005

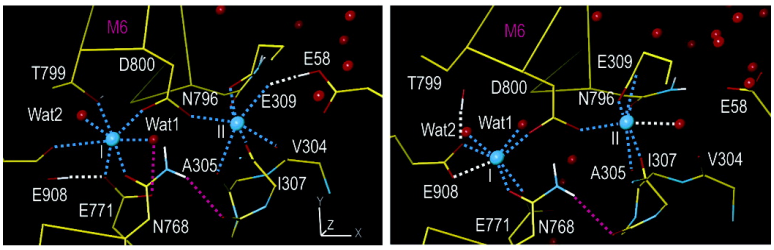

More About This Article

Additional resources and features associated with this article are available within the HTML version:

- Supporting Information
- Links to the 4 articles that cite this article, as of the time of this article download
- Access to high resolution figures
- Links to articles and content related to this article
- Copyright permission to reproduce figures and/or text from this article

View the Full Text HTML

J|A|C|S
COMMUNICATIONS

Published on Web 04/07/2005

Protonation of the Acidic Residues in the Transmembrane Cation-Binding Sites of the Ca^{2+} Pump

Yuji Sugita,[†] Naoyuki Miyashita,[†] Mitsunori Ikeguchi,[‡] Akinori Kidera,[‡] and Chikashi Toyoshima*,[†]

Institute of Molecular and Cellular Biosciences, The University of Tokyo, Yayoi 1-1-1, Bunkyo-ku, Tokyo 113-0032, Japan, and Graduate School of Integrated Science, Yokohama City University, Suehirocho 1-7-29, Tsurumi-ku, Yokohama, 230-0045, Japan

Received December 1, 2004; E-mail: ct@iam.u-tokyo.ac.jp

Sarcoplasmic reticulum (SR) Ca^{2+}-ATPase (SERCA1a) is an integral membrane protein of 110 kD and establishes a concentration gradient of Ca^{2+} across the SR membrane by transporting two Ca^{2+} per ATP hydrolyzed.[1] Recent X-ray structures of SR Ca^{2+}-ATPase in five different physiological states have revealed that large conformational changes occur during Ca^{2+} transport.[2−6] These X-ray structures also provide atomic models for two high-affinity Ca^{2+}-binding sites in the transmembrane region consisting of 10 helices (M1−M10).[2] In either site, Ca^{2+} is coordinated by seven oxygen atoms with different geometry. The first site (I in Figure 1a) consists of five side chain oxygen atoms of Asn768, Glu771, Thr799, Asp800, and Glu908, and two water molecules. Site II consists of four side chain oxygen atoms of Glu309, Asn796, and Asp800, and three backbone carbonyl oxygen atoms of Val304, Ala305, and Ile307. The geometry of site II is reminiscent of EF-hand, the most frequent Ca^{2+}-binding motif in soluble proteins. All these residues have been identified as critical by mutagenesis studies.[7]

Since many acidic residues cluster to form the Ca^{2+}-binding sites, side chain oxygen atoms inevitably come close to one another. In particular, the distance between the closest oxygen atoms of Glu58 and Glu309 is 2.44 Å, and that of Glu771 and Glu908 is 2.66 Å in an atomic model (PDB accession number, 1SU4)[2] of the Ca^{2+}-bound form. These short distances suggest that H-bonds are formed between them by protonation of the side chain oxygen. Ionization states of the acidic residues forming the Ca^{2+}-binding sites have particular importance, because Ca^{2+}-ATPase transports two or three protons in the direction opposite to Ca^{2+} (proton countertransport).[8] Here we examine their ionization states by evaluating the stabilization energy. We first address which residues become protonated at neutral pH; then we examine how the ionization states affect the stability of the Ca^{2+}-binding sites, which are located in the hydrophobic core of the bilayer.

Initially, continuum electrostatic calculations were carried out with the atomic model of the Ca^{2+}-bound form[2] to examine the ionization states of four Ca^{2+}-binding residues (Glu309, Glu771, Asp800, and Glu908) and Glu58 that is in close proximity to Glu309. For these, MEAD software package[9] was used. The dielectric constants for the solvent and the enzyme were assigned as 80 and 20, respectively. The lipid bilayer surrounding the enzyme was modeled as a slab of 30 Å thickness with the same dielectric constant as that assigned to the enzyme. In Figure 1b, the titration curves calculated for Glu58 and Glu908 show large positive shifts from that of Glu in solution (dotted curve), whereas little shift is shown for Glu771. In contrast, the titration curves for Glu309 and Asp800 show large negative shifts, reflecting that protonated forms of these acidic residues are more unfavorable than that in solution, because both of their carboxyl oxygen atoms directly coordinate

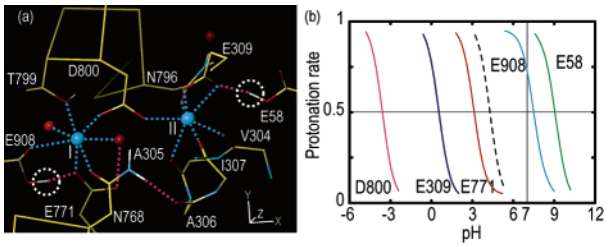

Figure 1. (a) Energy-minimized structure of the Ca^{2+}-binding sites viewed from the cytoplasmic side (approximately normal to the membrane). Cyan spheres represent Ca^{2+}, and red ones water. Dotted lines show the coordination of Ca^{2+} (cyan) and H-bonds (magenta). Protons bound to Glu58 and Glu908 are circled. Energy minimization was carried out with strong harmonic restraints (k = 1000.0 kcal/mol·Å^2) for all the heavy atoms of the enzyme. (b) Titration curves calculated for five acidic residues that form Ca^{2+}-binding sites of SR Ca^{2+}-ATPase as observed in the Ca^{2+}-bound structure shown in (a). Dashed line represents a reference titration curve calculated for a glutamic acid in solution.

Ca^{2+} at either site. The calculated protonation rates at pH = 7 are less than 1% for Glu309, Glu771, and Asp800, ∼74% for Glu908, and higher than 97% for Glu58, indicating that Glu58 and Glu908 are likely to be protonated. If we assign a dielectric constant of 4, which could be more appropriate for transmembrane part, the protonation rate of Glu58 and Glu908 becomes >99%. In Figure 1a, we show an energy-minimized structure of the Ca^{2+}-binding sites and the H-bond network. The H-bonds formed by protonation of Glu58 and Glu908 are likely to provide extra stability for the Ca^{2+}-binding sites while reducing electrostatic repulsion between the clustered acidic residues.

How the ionization states of Glu58 and Glu908 affect the stability of the Ca^{2+}-binding sites was studied further by all-atom molecular dynamics (MD) simulation with explicit solvent and lipids. As the enzyme reconstituted into dioleoylphosphatidyl-choline (DOPC) membrane shows similar ATPase activity to that in the native SR,[10] DOPC bilayer was generated first by MD simulation. The full system (Ca^{2+}-ATPase, 2 Ca^{2+}, 473 DOPC molecules, and salt solution) consisted of ∼276 000 atoms, including more than 65 000 water atoms. Here MARBLE software package[11] with CHARMM27 potential functions[12] was used for MD simulations at 1 atm and 310 K under constant area-isothermal isobaric (NPAT) conditions.[11,13] (See Supporting Information for more details.)

We carried out altogether seven MD simulations, two treating Glu58 and Glu908 protonated (MD1), three treating both of them unprotonated (MD2), and one each treating only one of them protonated (MD3). Each simulation consisted of 600-ps equilibration and 2-ns production dynamics (total time of seven simulations was more than 18 ns). In all the simulations, the three cytoplasmic domains as well as the transmembrane domain were stable (RMSD for Cα atoms was less than 1.6 Å from the starting structure). However, the stability of the Ca^{2+}-binding sites was substantially

[†] The University of Tokyo.
[‡] Yokohama City University.

10.1021/ja0427505 CCC: $30.25

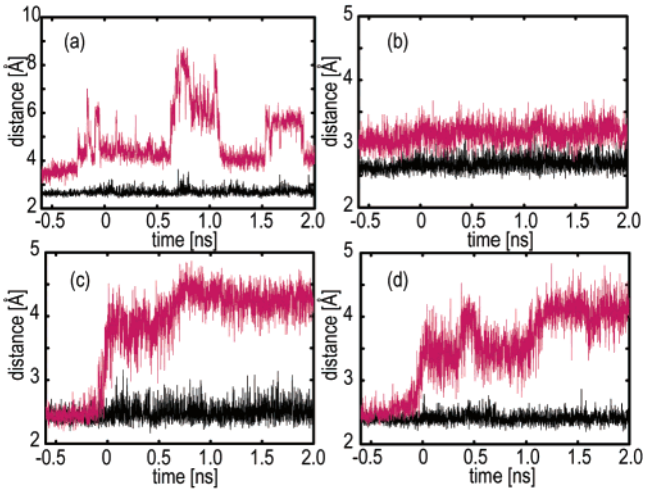

Figure 2. Time series of the characteristic distances around the Ca^{2+}-binding sites. Black and magenta lines represent the values obtained in MD1 and MD2 simulations, respectively. Distances are between the closest carboxyl oxygen atoms (a) in the side chains of Glu58 and Glu309 and (b) those of Glu771 and Glu908; (c) between site II Ca^{2+} and the carbonyl oxygen of Val304; (d) between site I Ca^{2+} and the side chain oxygen of Thr799.

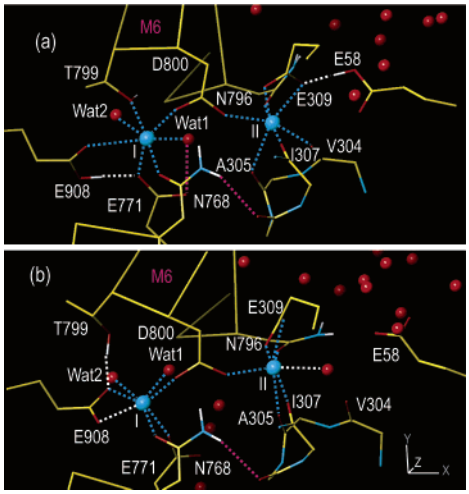

Figure 3. Snapshots of the Ca^{2+}-binding sites at the end of MD simulations. (a) MD1 in which Glu58 and Glu908 were modeled as protonated. (b) MD2 in which they were modeled as unprotonated. The binding sites are viewed from the same direction as that in Figure 1, and the atomic models were aligned by using all the Cα atoms in the M7−M10 helices. The dotted lines represent the Ca^{2+} coordinations (cyan) and the H-bond network (magenta). The white dotted lines indicate the bonds dependent on the protonation states.

different between the models with different protonation states. In Figure 2, we show time series of several distances that characterize the geometry of the Ca^{2+}-binding sites. In MD1, the geometry of Ca^{2+}-binding site and the H-bonds involving protonated carboxyls of Glu58 and Glu908 were stable throughout the 2-ns production dynamics (Figures 2 and 3a). An MD1 simulation was extended to 10 ns and confirmed the stability of the binding geometry.

In contrast, in MD2, the geometry was severely altered due to electrostatic repulsion between Glu58 and Glu309 and that between Glu771 and Glu908 (Figures 2 and 3b). Glu58 and Glu309 separated rapidly and then fluctuated independently, reflecting that the Glu58 side chain was not restrained by other residues (Figure 2a). The displacement of Glu58 yielded an empty space around site II Ca^{2+} to be filled with a water molecule from the cytoplasmic side. The water molecule coordinated site II Ca^{2+} in place of the backbone carbonyl of Val304 (Figure 2c). In contrast, the distance between Glu771 and Glu908 hardly changed in MD2 (Figure 2b), presumably because Glu908 side chain was fixed by its bidental binding to Ca^{2+} (Figure 3b). However, this position of Glu908 displaced Glu771, making the distance between them 0.5 Å longer than that in the crystal structure.[2] This change in Glu771 broke the H-bond with a water molecule coordinating site I Ca^{2+}, which in turn broke the Ca^{2+} coordination of Thr799 (Figure 2d). Thus, the difference in ionization of Glu58 and Glu908 altered the coordination geometry at the Ca^{2+}-binding sites, although seven-coordination of Ca^{2+} was maintained at either site. These alterations occurred independently of the other: when only one of the two residues was left ionized (MD3), the relevant binding site became broken. (See Supporting Information for more details.)

As described, the continuum electrostatic calculations and all-atom MD simulations consistently indicate that Glu58 and Glu908 are protonated at neutral pH and that protonation of these two acidic residues has important structural roles. Although no experimental measurements of pK_a are available for each acidic residue, the current results are totally consistent with prior mutagenesis works:[14,15] glutamine substitutions of Glu309 and Glu771 destroy the Ca^{2+} transport activity, whereas those of Glu58 and Glu908 do not. As the methods described here are readily applicable to atomic models of the Ca^{2+}-unbound state, they would be useful to understand the mechanism and roles of proton countertransport by Ca^{2+}-ATPase.

Acknowledgment. We are grateful to Prof. D. Bashford for providing us his MEAD software package. This work was supported, in part, by a Grant-in-Aid for Creative Science Research (C.T.) and for Scientific Research on Priority Areas (A) 'Membrane Interface' (Y.S.) from the Ministry of Education, Culture, Sports Science and Technology of Japan.

Supporting Information Available: Simulation methods and results, table of mean distances from the bound Ca^{2+} of coordinating atoms, structural model for SR Ca^{2+}-ATPase used in continuum electrostatic calculations, and snapshots of Ca^{2+}-binding sites at the end of MD simulations. This material is available free of charge via the Internet at http://pubs.acs.org.

References

(1) Møller, J. V.; Jull, B.; LeMaire, M. *Biochim. Biophys. Acta*. **1996**, *1286*, 1−51.
(2) Toyoshima, C.; Nakasako, M.; Nomura, H.; Ogawa, H. *Nature* **2000**, *405*, 647−655.
(3) Toyoshima, C.; Nomura, H. *Nature* **2002**, *418*, 605−611.
(4) Toyoshima, C.; Mizutani, T. *Nature* **2004**, *430*, 529−535.
(5) Toyoshima, C.; Nomura, H.; Tsuda, T. *Nature* **2004**, *432*, 361−368.
(6) Sørensen, T. L. M.; Møller, J. V.; Nissen, P. *Science* **2004**, *304*, 1672−1675.
(7) Clarke, D. M.; Loo, T. W.; Inesi, G.; MacLennan, D. H. *Nature* **1989**, *339*, 476−478.
(8) Yu, X.; Hao, L.; Inesi, G. *J. Biol. Chem.* **1994**, *269*, 16656−16661.
(9) Bashford, D.; Gerwert, K. *J. Mol. Biol.* **1992**, *224*, 473−486.
(10) Lee, A. G. *Biochim. Biophys. Acta* **1998**, *1376*, 381−390.
(11) Ikeguchi, M. *J. Comput. Chem.* **2004**, *25*, 529−541.
(12) MacKerell, A. D., Jr.; Bashford, D.; Bellott, M.; Dunbrack, R. L.; Evanseck, J. D.; Field, M. J.; Fischer, S.; Gao, J.; Guo, H.; Ha, S.; Joseph-McCarthy, D.; Kuchnir, L.; Kuczera, K.; Lau, F. T. K.; Mattos, C.; Michnick, S.; Ngo, T.; Nguyen, D. T.; Prodhom, B.; Reiher, W. E., III; Roux, B.; Schelenkrich, M.; Smith, J. C.; Stote, R.; Straub, J.; Watanabe, M.; Wiórkiewicz-Kuczera, J.; Yin, D.; Karplus, M. *J. Phys. Chem. B* **1998**, *102*, 3586−3616.
(13) Zhang, Y. H.; Feller, S. E.; Brooks, B. R.; Pastor, R. W. *J. Chem. Phys.* **1995**, *103*, 10252−10266.
(14) Zhang, Z.; Lewis, D.; Strock, C.; Inesi, G.; Nakasako, M.; Nomura, H.; Toyoshima, C. *Biochemistry* **2000**, *39*, 8758−8767.
(15) Clarke, D. M.; Maruyama, K.; Loo, T. W.; Leberer, E.; Inesi, G.; MacLennan, D. H. *J. Biol. Chem.* **1989**, *264*, 11246−11251.

JA0427505